



Modeling of enzymatic transesterification for omega-3 fatty acids enrichment in fish oil

M. Ongis^{a,b,*}, D. Liese^c, G. Di Marcoberardino^d, F. Gallucci^b, M. Binotti^{a,*}

^a Group of Energy Conversion Systems, Department of Energy, Politecnico di Milano, via Lambruschini 4a, 20156, Milano, Italy

^b Inorganic Membranes and Membrane Reactors, Sustainable Process Engineering, Department of Chemical Engineering and Chemistry, Eindhoven University of Technology, PO Box 513, 5600, MB, Eindhoven, The Netherlands

^c Enzymicals AG Walther-Rathenau-Straße 49a, 17489, Greifswald, Germany

^d Dipartimento di Ingegneria Meccanica e Industriale, Università degli Studi di Brescia, via Branze 38, 25123, Brescia, Italy

ARTICLE INFO

Keywords:

Modeling

Kinetics

Transesterification

Fish oil

Fatty acid enrichment

ABSTRACT

Mathematical models of transesterification commonly assume that oil is a mixture of triacylglycerols, where each component has only one type of acid attached. This article aims to show how a different assumption on acid distribution affects the results of acylglycerols fraction composition. Experiments of fish oil ethanolysis have been performed at different enzyme loadings and ethanol concentrations, leading to enrichments from 35 % to 52 % of ω 3 mass fraction in acylglycerols, by losing 12.1 % of ω 3 as ethyl esters. A kinetic model is developed assuming both all acids of the same type on each acylglycerol and all acids randomly distributed on the available positions. The two different assumptions showed strong discrepancies on the acylglycerols fraction compositions predictions, demonstrating how the initial fatty acids distribution is important when an accurate description of the acylglycerols fraction is desired.

1. Introduction

ω 3 polyunsaturated fatty acids (PUFAs) are nowadays the subject of several studies and reviews, due to the various benefits that their consumption can have on human health (Shahidi & Ambigaipalan, 2018). A review made by Khorshidi et al., 2023, shows the potentials of ω 3 in the reduction of triacylglycerols (TG) levels in young children and in people affected by hypertriglyceridemia. Another review reports their essential role in brain functions, improving learning, memory, cognitive well-being and blood flow in the brain (Dighriri et al., 2023). Other articles claim an anti-inflammatory capacity that can relieve pain and improve joint function in patients with osteoarthritis (Deng et al., 2023) and a capacity in lowering the risk of ovarian cancer (Zhang et al., 2023). Additional health benefits of these acids can be found in Lei et al., 2015; Chen et al., 2022.

Although the consumption of ω 3 through a balanced diet is typically suggested, when the availability of rich- ω 3 food is low, or in any other circumstance which could affect their consumption, people may benefit from ω 3 supplements (Dighriri et al., 2023). This led to an increasing interest in the medical and food industry on the production of edible supplements enriched in eicosapentaenoic (EPA) and docosahexaenoic

(DHA) acids, considered by several studies the responsible of the health benefits (Lei et al., 2015). Fish oil (by tuna, anchovies, sardines, cod livers, menhadens, trout or salmon) is the main source for these enriched products. The enrichment process of those oils allows to obtain a higher concentration of ω 3 reducing the content of other fatty acids, such as saturated fatty acids, that have been identified as one of the potential causes of obesity, hyperlipidaemia and atherosclerosis (Dong et al., 2023).

For these reasons, there is an undeniable interest in the research to find sustainable solutions for the fish oil enrichment process. Conventional enrichment process is the extraction of fish oil from fish waste by mincing, heating and centrifugation to separate the dried fish proteins from the oil (Fiori et al., 2014). Fish oil is then a mixture of TGs, and to separate the fatty acids it is necessary to detach them from the glycerol backbone, typically through transesterification with ethanol in the presence of an alkali catalyst, allowing an almost total conversion of the acids in ethyl ester (EE) form (Fiori et al., 2017). Ethyl esters can be then separated from each other through several technologies, such as molecular distillation, urea precipitation, supercritical fluid chromatography, supercritical fluid fractionation or a combination of them (Fiori et al., 2017). Another ω 3-enrichment process that is gaining an increasing interest is the enzymatic route (Jain et al., 2023; Marsol-Vall

* Corresponding authors at Group of Energy Conversion Systems, Department of Energy, Politecnico di Milano, via Lambruschini 4a, 20156 Milano, Italy.

E-mail addresses: michele.ongis@polimi.it (M. Ongis), marco.binotti@polimi.it (M. Binotti).

Nomenclature	
<i>MM</i>	Molar mass [g/mol]
<i>x</i>	Molar fraction [–]
<i>N</i>	Number of total types of fatty acids detected [–] or, in UD, number of different TG or DG types specified by subscript <i>k</i>
<i>conversion</i>	Fraction of acids converted into EE form [–]
<i>t</i>	Time [h]
<i>C</i>	Concentration [mM]
ϵ	Residual [mM]
<i>SSR</i>	Sum of the squared residuals [mM ²]
<i>R</i> ²	Coefficient of determination [–]
<i>SST</i>	Total sum of squares [mM ²]
<i>y</i>	Mass fraction [–]
<i>OE</i>	Oil enrichment [–]
<i>TR</i>	Target recovery [–]
<i>PI</i>	Performance index [–]
<i>rr</i>	Reaction rate [mM/h]
<i>P</i>	Probability of detachment [–]
<i>m</i>	Mass of enzyme beads loaded [g _{beads} / 50 mL _{sol}]
<i>k</i>	Reaction rate specific for unitary enzyme beads loading [(50 mL _{sol})/(mM•h•g _{beads})]
<i>a</i>	Coefficient in the exponent for the mathematical fitting expression of ϑ
<i>Greek symbols</i>	
ϑ	Reaction rate per unit concentrations of the reactants [1/(mM•h)]
ν	Stoichiometric coefficient [–]
ψ_{DG}^{TG}	Boolean variable to state if a specific DG can be obtained by a specific TG
ψ_{MG}^{DG}	Boolean variable to state if a specific MG can be obtained by a specific DG
δ	Higher acylglycerol in the UD to obtain the lower acylglycerol <i>z</i>
<i>Subscripts</i>	
<i>oil</i>	Relative to the fish oil
<i>i</i>	Relative to a specific fatty acid <i>i</i>
<i>gly</i>	Relative to glycerol
<i>H</i>	Relative to atomic hydrogen
<i>EtOH</i>	Relative to ethanol
<i>exp</i>	Experimental
<i>avg</i>	Average value
<i>EPA</i>	Relative to EPA
<i>DHA</i>	Relative to DHA
<i>EPA + DHA</i>	Relative to the enrichment of both EPA and DHA
<i>TG, DG, MG, EE</i>	In the simple model, relative to a component (not to its acids as in the case of superscripts) in that specific ester form
<i>G</i>	Relative to a generic acylglycerol
<i>HG</i>	Relative to a generic higher-acylglycerol
<i>LG</i>	Relative to a generic higher-acylglycerol
<i>f</i>	Relative to the forward reaction
<i>b</i>	Relative to the backward reaction
<i>d</i>	Relative to the inhibition term
<i>k</i>	Relative to a specific ester form in the simple model (<i>k</i> = <i>TG, DG, MG, EE</i>)
<i>z</i>	Relative to a generic component in the UD
<i>formed</i>	Relative to moles formed in the chemical reactions
<i>consumed</i>	Relative to moles consumed in the chemical reactions
<i>j</i>	In the model with UD, acid that should be detached from component δ to make <i>z</i>
<i>enzy</i>	Relative to the enzyme beads
<i>q</i>	Relative to ethanol volumetric fraction <i>q</i>
<i>R</i>	Fatty acid, in graphical representations
<i>Superscripts</i>	
<i>EE</i>	Relative to fatty acids in ethyl ester form
<i>TG</i>	Relative to fatty acids in triacylglycerol form
\wedge	Experimental value, measured
<i>DG</i>	Relative to fatty acids in diacylglycerol form
<i>MG</i>	Relative to fatty acids in monoacylglycerol form
<i>Abbreviations</i>	
PUFA	Polyunsaturated fatty acids
TG	Triacylglycerol
EPA	Eicosapentaenoic acid
DHA	Docosahexaenoic acid
EE	Ethyl ester
ME	Methyl ester
FFA	Free fatty acid
KPI	Key performance indicator
GC-FID	Gas chromatography – Flame ionization detector
FAME	Fatty acid methyl ester
SSR	Sum of the squared residuals
SST	Total sum of squares
DG	Diacylglycerol
MG	Monoacylglycerol
OE	Oil enrichment
TR	Target recovery
PI	Performance index
ODE	Ordinary differential equation

et al., 2022; Torres et al., 2002), where a lipase is able to detach selectively saturated and monounsaturated fatty acids from the glycerol backbone, leaving an acylglycerols fraction enriched in $\omega 3$ acids. This can be obtained through hydrolysis, producing free fatty acids (FFAs), or through alcoholysis (with ethanol or methanol), detaching acids as EEs or methyl esters (MEs). There are mainly two reasons for the interest in the enzymatic route: a product with PUFA in acylglycerols fraction, that could increase their bioavailability compared to having them as FFAs or EEs (Yang et al., 2020), and the simplicity to separate EEs (or FFAs) from the acylglycerols fraction. In this case, a separation is possible using polymeric membranes (Ghasemian et al., 2017). Enzymatic route coupled with membrane separation, from fish oil up to an enriched $\omega 3$ mixture, is currently under development in the European Union's funded project MACBETH, part of the Horizon 2020 program (Macbeth Project, 2019).

In this scenario, it is also increased the necessity of reliable mathematical models to describe the kinetics of the enzymatic reactions. Among the different enzyme-kinetic mechanisms developed (Ulus, 2015), the ping-pong bi-bi mechanism (with some variations such as considering the ethanol/water concentration constant or including the inverse reactions) is the most commonly used (Gog et al., 2012). Ping-pong bi-bi mechanism is a non-sequential mechanism that assumes the presence of two stable forms of the enzyme. The enzyme bounds with the acylglycerol (ping) and detach the fatty acids going to an acylated form, while the lower acylglycerol is released (pong). Then, ethanol is bounded to the acylated enzyme (ping), which produces the ethyl esters that is then released (pong), ending up again with the enzyme in its original nonacylated form. The history of the kinetic models for reactions similar to the ones investigated in this work is reported in Table 1. The rate equation for this mechanism is derived analytically in the work of

Table 1
Reaction rates of the kinetic models in literature for transesterification reactions.

Reference	Reaction	Kinetic Model	comments
		$r_i = \frac{\theta_1 \cdot C_G}{1 + \theta_2 \cdot C_G + \theta_3 \cdot C_G^2}$	General equation of the ping-pong bi-bi mechanism with backward reaction neglected
Malcata et al., 1992	Hydrolysis of butteroil	$r = \frac{\theta_1 \cdot C_G}{1 + \theta_2 \cdot C_G}$	Simplification (based on Cha's method) when deacylation is controlling and backward reaction neglected
		$r = \theta_1 \cdot C_G$	Simplification (based on Cha's method) when acylation is controlling and backward reaction neglected
		$r = \theta_1 \cdot C_G$	Acylation controlling and backward reaction neglected
Lessard & Hill, 2000a	Hydrolysis of butteroil	$r = \frac{\theta_1 \cdot C_G}{1 + \theta_2 \cdot C_G}$	Deacylation controlling and backward reaction neglected
Lessard & Hill, 2000b	Hydrolysis of butteroil	$r_i = \frac{\theta_{1,i} \cdot C_G}{1 + \sum_{i=1}^N \theta_{2,i} \cdot C_G}$	Deacylation controlling and backward reaction neglected in multi-response kinetics
		$r_i = \theta_{1,i} \cdot C_G \cdot C_{ETOH}$	Acylation controlling and without backward reaction
Torres et al., 2003	Ethanolysis of fish (menhaden) oil	$r_i = \frac{\theta_{1,i} \cdot C_{HG,i} \cdot C_{ETOH} - \theta_{2,i} \cdot C_{LG,i} \cdot C_{EE}}{1 + \sum_{i=1}^N \theta_{3,i} \cdot C_{HG,i}}$	Acylation controlling, Deacylation controlling, in multi response kinetics
Torres et al., 2004	Ethanolysis of borage oil	Same as in Torres et al., 2003	
		$r_{TG} = -\theta_{1,f} \cdot x_{TG} + \theta_{1,b} \cdot x_{DG} \cdot x_{EE}$	
		$r_{DG} = \theta_{1,f} \cdot x_{TG} - \theta_{1,b} \cdot x_{DG} \cdot x_{EE} - \theta_{2,f} \cdot x_{DG} + \theta_{2,b} \cdot x_{MG} \cdot x_{EE}$	Acylation controlling.
		$r_{MG} = \theta_{2,f} \cdot x_{DG} - \theta_{2,b} \cdot x_{MG} \cdot x_{EE} - \theta_{3,f} \cdot x_{MG} + \theta_{3,b} \cdot x_{Gly} \cdot x_{EE}$	Ethanol concentration not included in the equations.
		$r_{EE} = \theta_{1,f} \cdot x_{TG} - \theta_{1,b} \cdot x_{DG} \cdot x_{EE} + \theta_{2,f} \cdot x_{DG} - \theta_{2,b} \cdot x_{MG} \cdot x_{EE} + \theta_{3,f} \cdot x_{MG} - \theta_{3,b} \cdot x_{Gly} \cdot x_{EE}$	
		$r_{Gly} = \theta_{3,f} \cdot x_{MG} - \theta_{3,b} \cdot x_{Gly} \cdot x_{EE}$	
		Eqs. (9), (10), (11)	As in Torres et al., 2003, with acylation controlling
			As in Torres et al., 2003, with deacylation controlling. In supplementary materials.
This work	Ethanolysis of fish oil	Equations in supplementary materials	Uniform distribution of
		Eqs. (18), (19), (20)	

Table 1 (continued)

Reference	Reaction	Kinetic Model	comments
			the fatty acids assumed in the initial composition. Acylation is controlling.

Malcata et al., 1992, and considers a high number of parameters which can easily lead to overparameterization. For this reason, they proposed two simplified versions in which deacylation or acylation steps were considered as rate-limiting, ending up with simplified formulations of the model that showed the best fitting of the results. These simplifications can be derived using a method proposed by Cha, 1968 and derived from the method proposed by King & Altman, 1956. In the work of Cha, rate-limiting steps are identified in the enzyme-catalysed reactions, assuming other reaction steps in near-equilibrium conditions. This simplified formulation of the ping-pong bi-bi mechanism is a generalization of the original Michaelis-Menten mechanism, presented in a now classic article in 1913 (Michaelis & Menten, 1913) and recently translated by Johnson & Goody, 2011. In a more recent work of Torres et al., this simplified model of Malcata et al., 1992 was adapted to fish oil transesterification, showing that the backward reaction should be also considered (Torres et al., 2003). Moreover, it has been concluded that a simple first order power law in the reactants concentrations can be accurate enough to describe the process. This is also the approach selected for this work. The model ends up to be also the same used in the work of Bucio et al., 2015, but without using the assumption of constant ethanol concentration, since here the ethanol to oil ratio is several times lower than the one investigated in that work. Another version of the reaction rate equations, also investigated in the article of Torres et al., 2003, includes the inhibition term at the denominator, where the presence of other TGs could affect the enzyme ability to detach a specific acid. Also this formulation was investigated in this work, but results showed no significant improvement with respect to the formulation without inhibition term, as can be seen in supplementary materials.

It is a common assumption in scientific literature about modeling of enzymatic reaction to consider the TGs constituted by a glycerol backbone and three equal fatty acids (e.g. triolein, tripalmitin, etc...). This assumption is related to the fact that usually several acids can be detected and their possible combinations on the glycerol backbone would lead to a severely high number of compounds. However, this point is typically not properly discussed, nor it is its influence on the model predictions. Kinetic models are fitted on the experimental measurements of EEs detached, while the acids initial distribution can affect the composition of the acylglycerols fraction. This work aims to show how different assumptions on the initial fatty acids' distribution on the TGs available positions affect the modeling predictions on the acylglycerols fraction. The reaction investigated is fish oil transesterification with ethanol, using a selective lipase (CAL-A). Experiments are performed at different enzyme loadings and ethanol concentrations, to evaluate their influence on the reaction rates - as done in other articles for fish oil methanolysis (Jiang et al., 2023), fish oil ethanolysis using a simplified model (Bucio et al., 2015) and for kinetics of biodiesel production using ethanol (Calabrò et al., 2010) - and to optimize the Key Performance Indicators (KPIs), as defined in this article. A mathematical macro-kinetic model of the enzymatic reaction is fitted and validated on the experimental data. The model is used to properly quantify the selectivity of the enzyme, showed as different rate of release of the different acids in the oil, and to mathematically predict how the reaction rates change with enzyme loading and ethanol concentration. The kinetic model is developed in two variations: the former assumes, as typically in literature, same type of acid attached to any TG molecule. The latter, on the other hand, assumes a uniform distribution of the acids

on the available positions on the TG. The results of the two model variations are compared, showing how this assumption strongly affects the acylglycerols fraction composition predicted by the model.

2. Materials and methods

2.1. Materials

An immobilized formulation of *candida antarctica* lipase A (CAL-A) was chosen, and it was provided by Chiral Vision B.V. (The Netherlands). Fish (mainly anchovy) oil was provided by Solutex Corp (Spain), and it is a semi-refined oil, obtained by refining and bleaching raw oil. In this process, most of free fatty acids had been removed, and it was then determined through size-exclusion chromatography that more than 96 % of the acids are in the form of TGs. Therefore, in the oil model it is assumed for simplicity that all acids are, at the beginning, in form of TGs (an acid can be found attached to a TG, or attached to a diacylglycerol (DG) or to form a monoacylglycerol (MG). In all these cases, the acid is said to be in the acylglycerols fraction, since all these components are esters of glycerol. Lastly, it can be found as EE, which are esters of ethanol). Fish oil mass fractions has been determined through GC-FID analysis and is reported in Table 2. In the analyses, also traces of margaric acid (C17:0) and erucic acid (C22:1) have been detected: however their amount in the mixture was approximately 1.5 % of the total moles, thus it has been chosen to neglect them, in order to save computational time, and the other compounds fractions have been scaled up to 100 % maintaining the same relative fractions.

From the oil composition it is possible to determine the average molar mass of the fish oil. It is calculated as in eq. (1), where i represents the fatty acid, x_i its molar fraction, MM_i^{EE} its molar mass in the EE form and N is the number of fatty acids detected in the mixture (13 in this case). It resulted a molar mass of 307.42 g/mol.

$$MM_{oil}^{EE} = \sum_{i=1}^N x_i \cdot MM_i^{EE} \quad (1)$$

However, the molar mass of the oil in TG form is different from the molar mass of the oil assuming all the acids in EEs, mainly because one mole of TG is made up by three moles of EEs and a glycerol backbone. According to the transesterification reaction, it is possible to calculate the molar mass of the oil (assuming 100 % TG form) using eq. (2).

$$MM_{oil}^{TG} = (MM_{Gly} - 3 \cdot MM_H) + 3 \cdot (MM_{oil}^{EE} - (MM_{EtOH} - MM_H)) \quad (2)$$

Fish oil molar mass turns out to be 876.115 g/mol. The density of the selected fish oil is assumed equal to 930 g/L, while ethanol density resulted equal to 791 g/L at sampling conditions. These values have been used to calculate the molar concentrations of oil and ethanol in the

Table 2
Fish oil composition in terms of fatty acids.

Acid name	Acid index i	Acid code	Mass fraction	Mole fraction	Molar Mass as EE
(-)	(-)	(-)	(%)	(%)	(g/mol)
Myristic	1	C14:0	9.06	10.87	256.42
Palmitic	2	C16:0	19.29	20.85	284.47
Palmitoleic	3	C16:1	11.30	12.30	282.46
Stearic	4	C18:0	3.55	3.49	312.53
Oleic	5	C18:1	8.98	8.89	310.51
Octadecenoic	6	cis9	3.72	3.67	310.51
		cis11			
Linoleic	7	C18:2	1.33	1.32	308.49
Linolenic	8	C18:3	0.88	0.89	306.48
Arachidic	9	C20:0	3.83	3.45	340.58
Eicosenoic	10	C20:1	0.72	0.66	338.56
EPA	11	C20:5	20.91	19.45	330.50
DPA	12	C22:5	2.26	1.94	358.55
DHA	13	C22:6	14.15	12.20	356.54

experiments, while the total mixture volume (50 mL in all cases) is assumed to be constant at reaction temperature and throughout the process.

2.2. Experimental procedure

The experiments were carried out in batch mode on a 50 mL oil sample. First, the enzyme immobilized formulation was weighted and transferred into the flask. Fish oil was added and after five minutes of induction time ethanol, with different concentrations in different experiments, was added to the mixture. The reaction temperature was set to 40 °C. Samples were taken at defined time intervals and derivatized for analysis. Therefore, each sample was diluted with ethanol so that the ethanol oil ratio was set to 80:20. 100 μ L samples of this solution were divided into a 10 μ L sample for the EE analysis and a 90 μ L sample for total fatty acid content analysis. The 10 μ L EE sample was diluted with 330 μ L of ethanol to prepare the final sample for GC analysis. The 90 μ L sample for total fatty acid content analysis was diluted with 410 μ L of ethanol, sulfuric acid mixture (21 μ L 95 % sulfuric acid and 389 μ L ethanol) and was shaken at 1000 RPM at 60 °C for 180 min. Afterwards the solution was neutralized with 100 mg sodium carbonate and centrifuged to remove solid particles. After centrifugation, the sample was diluted 1:10 with ethanol to get the final sample for the GC analysis. GC-Analysis was performed on a Shimadzu Nexis 2030 with an FID detector. The column used for peak analysis was a FAME column from Agilent with a length of 100 m, film thickness 0.25 μ m and an inner diameter of 0.25 mm. Nitrogen was used as carrier gas with a linear velocity of 27.3 cm/s. The injector was at 270 °C, while the detector was set to 300 °C. 1 μ L of sample was injected with a 10:1 split ratio.

With this experimental procedure, it has been possible to measure, over time, the total acids amount and composition in each sample and the acids amount and composition in the EE form. The total amount of acids still attached to the acylglycerols can be therefore find from their difference. Amount of acids in EE form is used as basis for the model fitting and further validation.

2.3. Methodology

2.3.1. Experimental activity

The performed experiments aim at investigating the effect of ethanol concentration (between 7 % and 15 %) and of enzyme amount (from 0.5 to 5 g of beads) on the selective conversion of the different acids to EEs. Boundaries have been selected based on preliminary tests to avoid a reaction too fast or too slow, in case on enzyme, and to avoid negligible conversion (too low ethanol) from one side or phase separation (too much ethanol) on the other side.

Experiments 1 to 5 aim to investigate the effect of ethanol volumetric fraction (maintaining constant the enzyme amount and total mixture volume), while experiments 6 to 9 the effect of the enzyme beads loading (maintaining constant the ethanol volumetric fraction and the total mixture volume). Experiments 10 to 13 have been run to validate the kinetic model, with a new batch of both fish oil and enzyme, two for ethanol dependance (10 and 11) and two for enzyme dependance (12 and 13). A table where experiments conditions are summarized is available in supplementary materials.

In these experiments, the conversion of each acid in the mixture, defined as the ratio between the concentration of EEs of this specific acid $C_i^{EE}(t)$ over the total concentration of that acid in the mixture, in eq. (3), has been measured. To use the number of moles or the molar concentrations is in this case equivalent, since it is assumed that volume is constant throughout the reaction.

$$conversion_i(t) = \frac{C_i^{EE}(t)}{C_i^{TG}(t) + C_i^{DG}(t) + C_i^{MG}(t) + C_i^{EE}(t)} \quad (3)$$

2.3.2. Key performance indicators

Total conversion of fatty acids into EE form is defined in eq. (4). The conversion is important to understand how the overall reaction is proceeding, even if does not provide information about the enrichment process. It is analogous to the conversion of a single acid defined in eq. (3), but is relative to all the acids in the mixture.

$$\text{conversion}(t) = \frac{\sum_{i=1}^N C_i^{EE}(t)}{\sum_{i=1}^N (C_i^{TG}(t) + C_i^{DG}(t) + C_i^{MG}(t) + C_i^{EE}(t))} \quad (4)$$

Second indicator is called Oil Enrichment (OE) and it aims to evaluate the enrichment of the acylglycerols fraction in EPA and DHA compared to their mass fraction in the initial oil. OE is defined in eq. (5), where y represents the mass fraction, and it is a function of time.

$$OE(t) = \frac{y_{EPA+DHA}^{glycerides}(t)}{y_{EPA+DHA}^{oil\ TG}} \quad (5)$$

$$y_{EPA+DHA}^{glycerides}(t) = \frac{(C_{EPA}^{TG}(t) + C_{EPA}^{DG}(t) + C_{EPA}^{MG}(t)) \cdot MM_{EPA}^{EE} + (C_{DHA}^{TG}(t) + C_{DHA}^{DG}(t) + C_{DHA}^{MG}(t)) \cdot MM_{DHA}^{EE}}{\sum_{i=1}^{13} (C_i^{TG}(t) + C_i^{DG}(t) + C_i^{MG}(t)) \cdot MM_i^{EE}} \quad (6)$$

The initial mass fraction of EPA and DHA has been measured from oil composition, and is 35.06 %, where EPA is 20.91 % and DHA is 14.15 %, as shown in Table 2. This value is the constant OE denominator. The numerator of OE can be computed by calculating how many moles of EPA and DHA are attached to a glycerol backbone (so are in TG, DG or MG form), as reported in eq. (6). Molar masses of all acids as EEs can be found in Table 2, while molar concentrations over time are outputs of the model.

Another important parameter to be taken into account is related to the fact that, as time passes, even if the enrichment increases over time, more and more EPA and DHA go to the EE fraction. Since they are not in the final mixture of acylglycerols, it represents a loss. To evaluate this effect, a KPI called Target Recovery (TR) is defined, in eq. (7), as the ratio between EPA and DHA moles in acylglycerols and their total amount in the fed oil.

$$\begin{aligned} TR(t) &= \frac{C_{EPA}^{TG}(t) + C_{EPA}^{DG}(t) + C_{EPA}^{MG}(t) + C_{DHA}^{TG}(t) + C_{DHA}^{DG}(t) + C_{DHA}^{MG}(t)}{C_{EPA}^{oil\ TG} + C_{DHA}^{oil\ TG}} \\ &= 1 - \frac{C_{EPA}^{EE}(t) + C_{DHA}^{EE}(t)}{C_{EPA}^{oil\ TG} + C_{DHA}^{oil\ TG}} \end{aligned} \quad (7)$$

A value, for example, of 90 % means that 90 % of the total moles of EPA and DHA are still in the acylglycerols fraction, while 10 % have been detached and converted to EEs.

To consider both the effects together, an index called Performance Index (PI) is defined as the product between oil enrichment and target recovery.

$$PI(t) = OE(t) \cdot TR(t) \quad (8)$$

The process optimization aims at maximizing the PI as function of time and of ethanol fraction.

3. Mathematical modeling

3.1. Generalities on the kinetic models

In this work, the assumed set of reaction is the following:



where the detailed reaction description of each acid involved in these reactions depend on the assumptions of the distribution of the TGs in the fish oil, as it will be presented in sections 3.2 and 3.3. Two different approach are here considered and investigated: the Selective Distribution (SD) model, as presented in section 3.2, in line with what can be found in literature, assumes that only acids of the same type are attached to a specific acylglycerol; the Uniform Distribution (UD) model, proposed in section 3.3, assumes that acids are randomly distributed on the TGs. The goal is to assess how the resulting distribution of the target $\omega 3$

in the product is affected by the assumptions on the acids' distribution in the reactants (i.e. TGs). An example to show the difference between the two models is reported in Fig. 1, considering for simplicity only 3 acids involved (while in this case study there are 13). It is worth mentioning that in both models it is assumed that the acid position in the acylglycerol (e.g., center or side in a TG) has no influence on the enzyme ability to detach it, as is reported in literature that CAL-A has no particular regioselectivity (Akanbi & Barrow, 2017; He et al., 2016).

3.2. Selective distribution in the kinetic model

SD distribution makes the strong assumption that all the acids attached to a certain acylglycerol (TG and DG) are the same type of acid. In this case, the molar concentration of each acid in the oil, at the reactor inlet, corresponds exactly to the molar fractions of the different TGs. It is possible to associate to each acid the corresponding ester, which can then be identified with the subscript i to a specific acid. Since there are 13 acids in the investigated oil ($N = 13$), the components involved will be 13 TGs, 13 DGs, 13 MGs, 13 EEs, ethanol and glycerol, for a total of 54 components. The generic acylglycerol of interest can be identified by the letter k . The notation adopted to represent the concentration of a component is $C_{i,k}$, representing the concentration of the component in the ester form k with attached the acid i . Then, for example, $C_{1,DG}$ identifies the (molar) concentration of DG formed with myristic acid (that is, glycerol backbone with two myristic acids attached). It is worth mentioning that this notation differs from the other notation previously used in the definitions of KPIs, that is C_i^k . The latter represents the concentration of the fatty acid i that can be found in the acylglycerol k . Using the same example, C_1^{DG} is the concentration of myristic acid that can be found in DG form. It can be easily stated that $C_1^{DG} = 2 \cdot C_{1,DG}$, since there are two moles of myristic acid per mole of DG. In case of a TG, the coefficient is 3, while for a MG and an EE is 1, so numerically there is no difference (even if there is conceptually).

Following the previous section, the reaction rates of the reaction R.1, R.2 and R.3, for each involved acid, are defined in eqs. (9), (10) and (11) with a second order kinetic. Absolute values of the stoichiometric

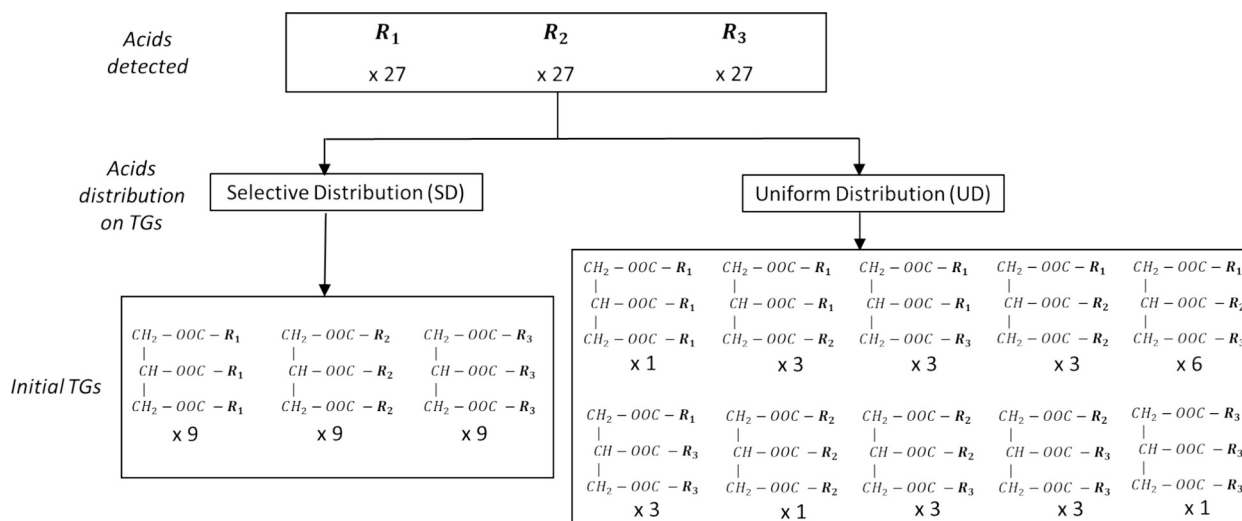


Fig. 1. difference between SD and UD assumptions in the kinetic model. Example of distribution of three fatty acids (R_1 , R_2 and R_3) on the available positions of the TGs in the fish oil before reaction. It is assumed that position on the TG has no influence (combinations are considered instead of dispositions).

coefficient $\nu_{i,k}$ is always equal to 1, unless the component $C_{i,k}$ is not involved in the reaction: in this latter case it is equal to zero and reaction rate cannot then be defined.

$$\begin{aligned} r_{i,R,1}(t) &= \frac{1}{|\nu_{i,k,R,1}|} \left. \frac{dC_{i,k}(t)}{dt} \right|_{R,1} \\ &= \vartheta_{i,f,R,1} \cdot C_{i,TG}(t) \cdot C_{EtOH}(t) - \vartheta_{i,b,R,1} \cdot C_{i,DG}(t) \cdot C_{i,EE}(t) \end{aligned} \quad (9)$$

$$\begin{aligned} r_{i,R,2}(t) &= \frac{1}{|\nu_{i,k,R,2}|} \left. \frac{dC_{i,k}(t)}{dt} \right|_{R,2} \\ &= \vartheta_{i,f,R,2} \cdot C_{i,DG}(t) \cdot C_{EtOH}(t) - \vartheta_{i,b,R,2} \cdot C_{i,MG}(t) \cdot C_{i,EE}(t) \end{aligned} \quad (10)$$

$$\begin{aligned} r_{i,R,3}(t) &= \frac{1}{|\nu_{i,k,R,3}|} \left. \frac{dC_{i,k}(t)}{dt} \right|_{R,3} \\ &= \vartheta_{i,f,R,3} \cdot C_{i,MG}(t) \cdot C_{EtOH}(t) - \vartheta_{i,b,R,3} \cdot C_{Gly}(t) \cdot C_{i,EE}(t) \end{aligned} \quad (11)$$

In these equations, ϑ_i represents the reaction rate for unit concentrations of the reactants, for the forward f and the backward b reactions of each reaction $R.1$, $R.2$ and $R.3$. In this analysis, it is assumed that these parameters, related to the ability of the enzyme to detach a certain acid, are not dependent on the ester form involved. In other words, it is assumed that the enzyme has the same ability to detach a specific acid from a TG, from a DG or from a MG. Mathematically, it means that $\vartheta_{i,f,R,1} = \vartheta_{i,f,R,2} = \vartheta_{i,f,R,3} = \vartheta_{i,f}$ and $\vartheta_{i,b,R,1} = \vartheta_{i,b,R,2} = \vartheta_{i,b,R,3} = \vartheta_{i,b}$. The parameters $\vartheta_{i,f}$ and $\vartheta_{i,b}$ are fitted, for each component, based on the experimental data.

Once calculated the rate equations, the model solves the material balances for all the components involved by solving the following ordinary differential equations' (ODE) system through the function *ode45* in Matlab®. Eq. (12) represents the material balance for the 52 esters, while (13) and (14) the material balances for ethanol and glycerol respectively. Together they form a system of 54 ODEs. The Cauchy's problem can be solved by imposing the concentrations at time $t = 0$, which are known from oil composition and experimental conditions.

$$\frac{dC_{i,k}(t)}{dt} = \nu_{i,k,R,1} \cdot r_{i,R,1}(t) + \nu_{i,k,R,2} \cdot r_{i,R,2}(t) + \nu_{i,k,R,3} \cdot r_{i,R,3}(t) \quad (12)$$

$$\frac{dC_{EtOH}(t)}{dt} = - \sum_{i=1}^N r_{i,R,1}(t) - \sum_{i=1}^N r_{i,R,2}(t) - \sum_{i=1}^N r_{i,R,3}(t) \quad (13)$$

$$\frac{dC_{Gly}(t)}{dt} = \sum_{i=1}^N r_{i,R,3}(t) \quad (14)$$

The parameter $\nu_{i,k}$ represents the stoichiometric coefficient of the component made by acid i in the ester form k specific to a certain reaction, and it can be $+1$ if the component is a product, -1 if it is a reactant and 0 if it is not involved in that reaction.

3.3. Uniform distribution in the kinetic model

The model proposed in section 3.2 is a first step to describe the fish oil ethanolsis. It is however based on a strong assumption, typically assumed also in the scientific literature, that only one type of acid can be attached to any specific ester. This is very unlikely to happen in the real world and could lead to an overestimation of the TG fraction, thus underestimating DG and MG fractions, even if correctly fitted on EEs data. This risk of a wrong description of the acylglycerols fraction is conceptually presented through an example in the supplementary materials. On the other hand, to understand how the fatty acids are distributed on the different TGs can be experimentally difficult and inconvenient, especially in case there are many different fatty acids in the mixture.

Therefore, the approach proposed in this article is to investigate the differences that can be obtained assuming a uniform distribution of the fatty acids, among the available positions in the fish oil TGs. Since there is a different (but precise) number of moles of acid of each type, the amount of each TG produced will be dependent on the quantity of each acid. The molar fraction of each possible TG is calculated in Matlab®, by randomly distributing a vast number of fatty acids molecules (with the same molar fraction as in the feed) in three different positions with uniform distribution, using the *rand* function.

The UD leads to a larger number of TG types, and it is surely more complex than the SD. However, it is also more likely that the UD represents the reality better than the strong assumption of the SD.

In the UD, the number of possible combinations of acids in TGs, DGs and MGs can be found from eqs. (15), (16) and (17) respectively, according to the reactions defined in section 3.1.

$$N_{TG} = \frac{(N+2)!}{3! \cdot (N-1)!} \quad (15)$$

$$N_{DG} = \frac{(N+1)!}{2! \cdot (N-1)!} \quad (16)$$

$$N_{MG} = N \quad (17)$$

where N is the number of fatty acids. In this case, with 13 acids, it turns out that there are 455 different TGs and 91 DGs, while of course 13 MGs and 13 EEs, since there is only one acid attached. Including ethanol and glycerol, it leads to a system of 574 ODEs to be solved over time. However, the computational effort due to higher number of equations is not the only additional complexity compared to the SD. In this model, it should be considered that a certain TG can lead only to some specific DGs, and, among the possible DGs that can be obtained, the amount of each type of DG depends on the acids initially attached and to the probability of detaching each one of these acids. To describe this process, the mathematical problem is formulated as follows.

Reaction rates are similar to the ones presented in eqs. (9), (10) and (11). However, this time it is not possible to refer to the component $C_{i,k}$, since there is no more correspondence between acid and component. The reaction rates are here referred to the overall concentration of the acid type i in a certain ester form C_i^k . This leads to eqs. (18), (19) and (20):

$$rr_{i,R.1}(t) = \frac{dC_i^{EE}(t)}{dt} \Big|_{R.1} = \vartheta_{i,f} \cdot C_i^{TG}(t) \cdot C_{EtOH}(t) - \vartheta_{i,b} \cdot C_i^{DG}(t) \cdot C_i^{EE}(t) \quad (18)$$

$$rr_{i,R.2}(t) = \frac{dC_i^{EE}(t)}{dt} \Big|_{R.2} = \vartheta_{i,f} \cdot C_i^{DG}(t) \cdot C_{EtOH}(t) - \vartheta_{i,b} \cdot C_i^{MG}(t) \cdot C_i^{EE}(t) \quad (19)$$

$$rr_{i,R.3}(t) = \frac{dC_i^{EE}(t)}{dt} \Big|_{R.3} = \vartheta_{i,f} \cdot C_i^{MG}(t) \cdot C_{EtOH}(t) - \vartheta_{i,b} \cdot C_{Gly}(t) \cdot C_i^{EE}(t) \quad (20)$$

In this context, the definition of reaction rate represents the derivative of the concentration of acids i in the form k . It is then a measure of all the acids of type i detached from the glycerol backbones of the different acylglycerols where they came from.

To evaluate the material balances a further assumption is needed: it is assumed that the enzyme does not discriminate if a specific acid is attached with different acids, and then all the fatty acids of a specific type have the same probability to be detached. It consequently follows that if a component has 3 EPA attached, then it has three times the probability that EPA will be detached from that component compared to the probability that it is detached from a component with only one EPA. To evaluate from which components are they detached, a *probability of detachment* $P_{z,i}^k$ function is defined as in eq. (21) for all the components. Such function assumes that the probability to detach one specific acid i from one generic component z is proportional to the number of that acid attached to that specific component $C_{i,z}$ over the total number of acids of the same type i attached to all the components that are in the same ester form. If, for example, there is a TG with two EPAs and one oleic acid, its probability function for EPA (to know which percentage of EPA detached, given by its reaction rate, are detached from this component) can be calculated from the concentration of EPA in that component (that is, two times the concentration of the component itself) over the total concentration of EPA attached to all the TGs.

$$P_{z,i}^k(t) = \frac{C_{i,z}^k(t)}{\sum_{\text{all } z \text{ in } k} C_{i,z}^k(t)} \quad (21)$$

Material balances for TGs, EEs, ethanol and glycerol can already be stated:

$$\frac{dC_z^{TG}(t)}{dt} = - \sum_{i=1}^N P_{z,i}^{TG}(t) \cdot rr_{i,R.1}(t) \quad (22)$$

$$\frac{dC_z^{EE}(t)}{dt} = rr_{i,R.1}(t) + rr_{i,R.2}(t) + rr_{i,R.3}(t) \quad (23)$$

$$\frac{dC_{EtOH}(t)}{dt} = - \sum_{i=1}^N rr_{i,R.1}(t) - \sum_{i=1}^N rr_{i,R.2}(t) - \sum_{i=1}^N rr_{i,R.3}(t) \quad (24)$$

$$\frac{dC_{Gly}(t)}{dt} = \sum_{i=1}^N rr_{i,R.3}(t) \quad (25)$$

Eq. (22) represents the material balance for TGs, which are 455 components. To evaluate how changes the concentration of each component in TG form C_z^{TG} , for all the acids, the amount of each acid detached can be found by multiplying the reaction rate of that acid in reaction R.1 (which represents the total number of acids detached from all TGs) multiplied by the probability function of that acid in that component (which represents the percentage of acid detached allocated to that component). The probability is zero if the acid i is not present on the considered component z . In eq. (23) there is a correspondence between z (the component) and i (the acid), since only one acid forms the specific EE. Then of course, it should be used the reaction rate of the acid that is the same acid which forms the ethyl ester z .

To evaluate the material balances for components in DG and MG forms, an additional parameter is introduced. While the number of acids detached from each component in this form can be calculated as previously done for TGs, the DGs formed at each step depend on the components obtained from the previous detachment of acids from the TGs. The same can be said for MGs. The material balances can be represented as:

$$\frac{dC_z^{DG}(t)}{dt} = \frac{dC_{z,formed}^{DG}(t)}{dt} - \frac{dC_{z,consumed}^{DG}(t)}{dt} \quad (26)$$

$$\frac{dC_z^{MG}(t)}{dt} = \frac{dC_{z,formed}^{MG}(t)}{dt} - \frac{dC_{z,consumed}^{MG}(t)}{dt} \quad (27)$$

where the amount that is consumed can be calculated for DGs as already made for TGs. For MGs it is not necessary to use the probability function, since its values are always equal to 1 (there is only one acid associated to each MG).

$$\frac{dC_{z,consumed}^{DG}(t)}{dt} = \sum_{i=1}^N P_{z,i}^{DG}(t) \cdot rr_{i,R.2}(t) \quad (28)$$

$$\frac{dC_{z,consumed}^{MG}(t)}{dt} = \sum_{i=1}^N rr_{i,R.3}(t) \quad (29)$$

The amount of each component that is formed from the detachment of an acid from the upper-order acylglycerol can be calculated by introducing the parameter ψ_{DG}^{TG} . This parameter is introduced to mathematically state the possibility to obtain a specific DG starting from any specific TG. ψ_{DG}^{TG} is 1 if the considered DG can be produced starting from the considered TG, 0 otherwise. The acid that should be detached from the TG to make the DG z is identified with the letter j . It can be stated then:

$$\frac{dC_{z,formed}^{DG}(t)}{dt} = \sum_{\text{all TGs } \delta} \psi_{DG}^{TG} \cdot rr_{j,R.1}(t) \cdot P_{\delta,j}^{TG}(t) \quad (30)$$

In other words, for each TG it is checked if that component can or cannot form the DG of interest, and then it is estimated how many moles of acid j (the one to be detached from that TG to make the DG of interest) are detached. The same idea can be applied to the formation of MGs, this time considering DGs as the components to start from.

$$\frac{dC_{z,formed}^{MG}(t)}{dt} = \sum_{\text{all DGs } \delta} \psi_{MG}^{DG} \cdot rr_{j,R.2}(t) \cdot P_{\delta,j}^{DG}(t) \quad (31)$$

With eqs. (30) and (31) the material balances can be completed. Eqs. (22) to (31) can be combined in a system of 574 ODEs. Together with their initial values, which are known from the experimental conditions

of the mixture fed (amount of ethanol, amount and composition of oil of the specific experiment), the Cauchy's problem can be solved.

3.4. Model fitting

In the experimental activity, the concentration of each fatty acid i , named $\hat{C}_i^{EE}(t)$, has been measured over time, typically through 10 samples along 23 h. The residual of acid i at time t , called $e_i(t)$, is defined as the difference between the value of the concentration predicted by the model $C_i^{EE}(t)$ - that is equivalent to $C_z^{EE}(t)$ in the UD - and the experimental measurement $\hat{C}_i^{EE}(t)$. For both SD and UD, the concentrations of all acids over time are determined once set their initial values and the parameters $\vartheta_{i,f}$ and $\vartheta_{i,b}$ for all the involved fatty acids.

The kinetic model parameters $\vartheta_{i,f}$ and $\vartheta_{i,b}$ have been fitted by minimizing the Sum of the Squares Residuals (SSR) of all the experimental points of all acids. Definition of SSR is reported in eq. (32). This residual minimization has been performed in Matlab® using the function *fmincon*. In other words, the software provides the values of $\vartheta_{i,f}$ and $\vartheta_{i,b}$ of all acids that minimizes sum of the squared residuals for all acids for all the experimental point, making then a global minimization.

$$SSR = \sum_{t=0}^{t_{exp}} \sum_{i=1}^N e_i^2(t) = \sum_{t=0}^{t_{exp}} \sum_{i=1}^N (C_i^{EE}(t) - \hat{C}_i^{EE}(t))^2 \quad (32)$$

However, the fitting of 26 parameters (13 for the $\vartheta_{i,f}$ and 13 for the $\vartheta_{i,b}$) together can be complex from a computational point of view and with considerable risk of overparameterization. Thus, a simplified approach has been used in this work. Based on preliminary experimental results, it has been noticed that some acids showed the same conversion (or a fixed percentage of the conversion of another acid) over time. This was verified for all the experiments performed. Based on this observation, the components were grouped in five classes with similar conversion trend and for each class the most abundant component was selected to describe the conversion of the entire class. This approach reduces the degree of complexity of the problem, requiring to fit only 10 parameters (2 for 5 acids). These representative components - C16:0, C16:1, C18:1 cis11, EPA, DHA - are approximately 70 % of the total acids moles of the mixture. The concentration of the other 8 components (C14:0; C18:0; C18:1cis9; C18:2; C18:3; C20:0; C20:1; C22:5) is computed by the model, starting from the parameters $\vartheta_{i,f}$ and $\vartheta_{i,b}$ of the five components fitted. More details on the grouping procedure and on its impact on the overall results is reported in supplementary materials, and one example of the fitting result for one experiment can be seen in Fig. 2.

Once fitted the parameters, the quality of the fitting is evaluated using the R^2 index, also called coefficient of determination, calculated according to the definition in eq. (33).

$$R^2 = 1 - \frac{SSR}{SST} \quad (33)$$

where SST is defined as in eq. (34), and is the Total Sum of the Squares (SST), which is defined as the overall sum of the squared difference between experimental results and the average of the experimental results specific to a component $\hat{C}_{i,avg}^{EE}$, given by the sum of all concentrations of acid i over time divided by the number of experimental points.

$$SST = \sum_{t=0}^{t_{exp}} \sum_{i=1}^N (\hat{C}_i^{EE}(t) - \hat{C}_{i,avg}^{EE})^2 \quad (34)$$

The comparison between values of R^2 resulting from the fittings of SD and UD can be found in Fig. 5.

4. Results and discussion

Once defined materials and methods in section 2 and the mathematical models in section 3, in this section both experimental and

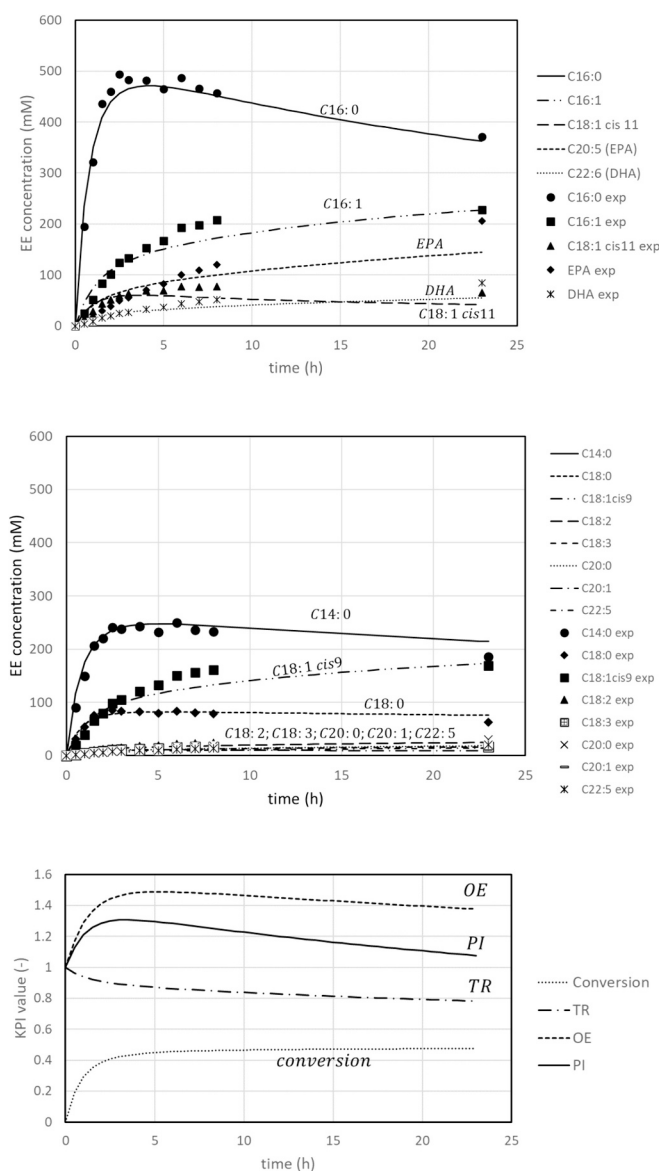


Fig. 2. Trends of concentrations of EEs of different fatty acids over time in experiment 8, divided between the fitted components (top) and the other components which conversion is calculated from the fitted ones (middle). On the bottom, trend of KPIs for experiment 8.

modeling results are presented and discussed. Since the fitting of the SD and the UD are based on the same data, the generalities on experimental results and system behavior are presented in the SD section only, while a comparison between the two approaches is reported in the description of UD.

4.1. SD in the kinetic model

4.1.1. Trends of concentrations and key performance indicators in one experiment

Typical trends of the EE concentrations, divided per fitted acids, are reported in Fig. 2. The lines represent the model prediction obtained once the values of $\vartheta_{i,f}$ and $\vartheta_{i,b}$ have been fitted for the specific experiment, while the marker the experimental measurements. The top figure represents the typical profile of the concentrations of the ethyl esters of the five fitted acids over time. It appears clear how the enzyme detaches preferably short-chain acids and leaves EPA and DHA attached, therefore their concentration as EEs is low. As time passes, some components

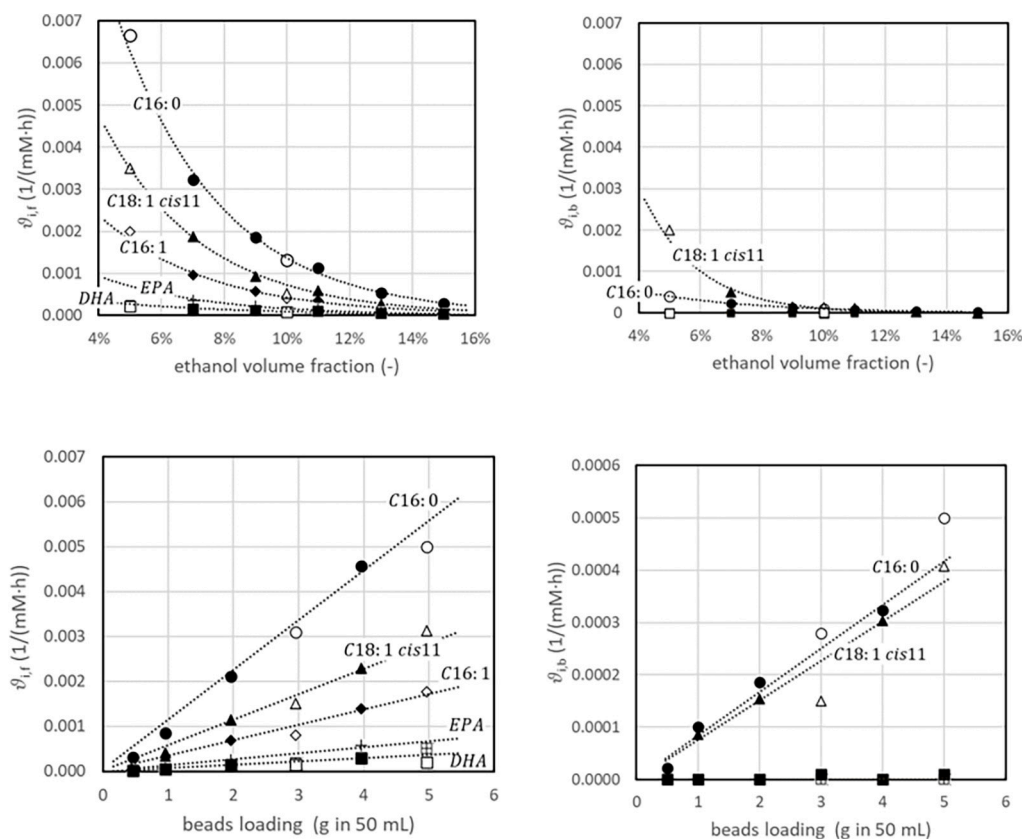


Fig. 3. $\vartheta_{i,f}$ and $\vartheta_{i,b}$ for different ethanol volume fraction (top) and for different beads loading (bottom). Experimental data used to fit the model coefficient (black markers, experiment #1–9) and experimental data used for validation (with markers, experiment #10–13). Model results are reported with dotted lines. (●) C16:0 exp. for fitting; (○) C16:0 exp. for validation; (◆) C16:1 exp. for fitting; (◇) C16:1 exp. for validation; (▲) C18:1cis11 exp. for fitting; (△) C18:1cis11 exp. for validation; (+) EPA exp. for fitting; (⊞) EPA exp. for validation; (■) DHA exp. for fitting; (□) DHA exp. for validation.

(C16:0, C18:1 cis11) reach a peak and then concentration decreases. This is due to re-attachment to the EEs to their acylglycerols, since also the inverse reaction is occurring. At the center, the trend of the other 8 components is shown: the concentrations are based on the values of $\vartheta_{i,f}$ and $\vartheta_{i,b}$ that are not directly fitted, as for the main components, but are calculated as a fixed percentage of the $\vartheta_{i,f}$ and $\vartheta_{i,b}$ of the fitted components. The goodness of this prediction allows to validate a posteriori the assumption stated in section 3.2 to fit only five main components in order to save computational time. The considerations on their trends are the same as for the fitted components. It is also possible to compute and plot the KPIs, defined in section 2.3.2. The resulting trends over time are presented at the bottom of Fig. 2.

The easiest trend to explain is the one of TR, representing the ratio between the $\omega 3$ moles still attached to the glycerol backbone, and the total amount of $\omega 3$ in the mixture (so, the numerator plus the amount of $\omega 3$ in EEs). Its value starts from one, since at the beginning all acids are in TG form, and then it continuously decreases as more $\omega 3$ are detached. The other parameter, OE, represents the ratio between the mass fraction of $\omega 3$ in the acylglycerols fraction and the mass fraction in the initial oil. As shown in Fig. 3 (bottom), it increases at the beginning, reaches a maximum and then slowly decreases. The reason for this trend, which is also followed by the PI, is that at the beginning the enzyme detaches selectively most of the acids, which concentration as EEs increase steeply. After a while, due to the high number of EEs available in the mixture, they start to recombine and to form acylglycerols. In Fig. 2, for example, this is the case for C16:0, C14:0 and C18:1 cis11. These behaviors lead to the presence of a maximum of the PI, which represents the optimum time where the reaction should be stopped. Another interesting trend is the one of total conversion, which is the percentage of acids converted to EEs. In experiment 9, about 47.5 % of the acids are

detached over time. It is interesting the fact that overall, the conversion reaches an equilibrium and so the number of EEs is stable over time, after an initial transient. However, looking inside the different fatty acids which compose the EEs fraction, they are changing proportion over time. In other words, the different acids are rearranging themselves on the acylglycerols available positions, while maintaining the total number of detached acids constant.

4.1.2. Parameters fitting and model validation

The quality of the fitting on the five acids representative of the five classes of components is expressed in terms of R^2 index, as defined in equation). Results are reported in Fig. 5, in comparison with the UD. However, in all cases the index is above 0.9, which suggests a good fitting.

In Fig. 3, the values of $\vartheta_{i,f}$ (left figures) and $\vartheta_{i,b}$ (right figures) in two set of experiments on ethanol concentration (top figures) and on enzyme beads loading (bottom figures) are reported. In the case of ethanol fraction, the trend of both $\vartheta_{i,f}$ and $\vartheta_{i,b}$ is exponential for all components. In case of beads loading, the trend is linear, and in particular $\vartheta_{i,f}$ and $\vartheta_{i,b}$ are, for all components, proportional to the beads loading, due to the proportional additional availability of active sites on the lipase. These results allow to write the reaction rates specific for beads grams, namely $\vartheta_{i,f} = k_{i,f} \cdot m_{enzyme}$ and $\vartheta_{i,b} = k_{i,b} \cdot m_{enzyme}$, where m_{enzyme} are the grams of beads per 50 mL of solution. To validate the model, the results of experiments 10 to 13 are also reported in Fig. 3 (empty indicators).

Results of the validation show that the model can reproduce the experimental results obtained with a new oil batch (thus with a slightly different composition in terms of fatty acids compare to the one used for fitting). The goodness of the prediction is verified also for values outside the fitting range, as in the case of the experiment with 5 % of ethanol and

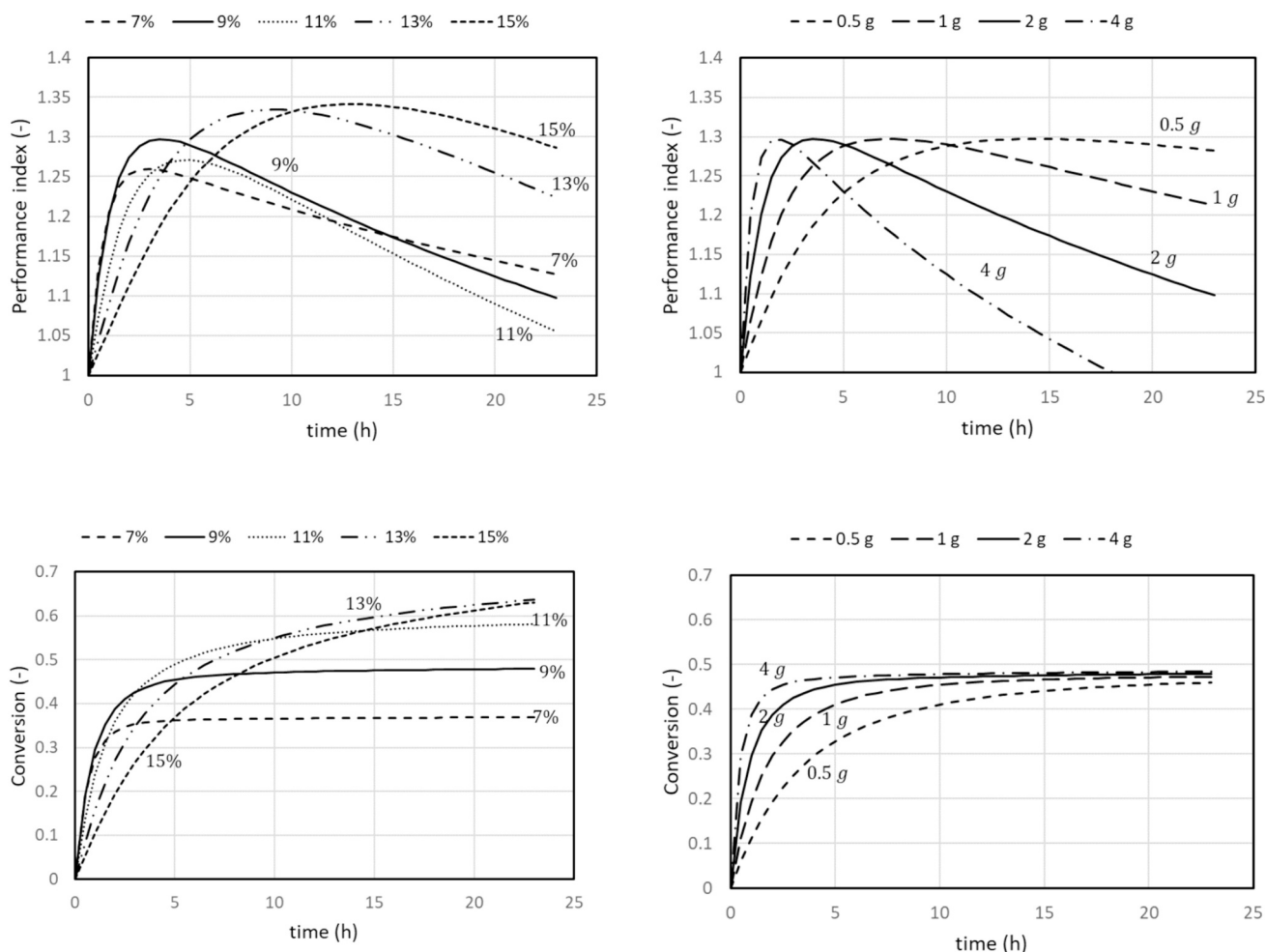


Fig. 4. trend of PI (top) and conversion (bottom) over time in the different experiments. On the left, ethanol influence (fitting based on experiments 1 to 5). On the right, enzyme amount influence (fitting based on experiments 6 to 9).

the experiment with 5 g of enzyme.

Regarding ethanol trend, it should be mentioned however that the exponential behavior does not hold for extremely low concentration because, as already obtained by [Jiang et al., 2023](#) for methanolysis, at very low ethanol concentration no conversion can be obtained and the values of ϑ_{if} and ϑ_{ib} should steeply drop to zero.

Some deviations can be observed in the backward parameters in the enzyme-related experiments. However, it is worth mentioning that their influence on the overall fitting quality, compared to the one of the fitting the parameters of the forward reaction, is quite limited. As shown in [Fig. 3](#), they resulted in general one order of magnitude lower than the forward reaction parameters.

4.1.3. Trends of KPIs in all experiments

The effect of ethanol concentration (left) and enzyme amount (right) on PI (top) and on conversion (bottom) is reported in [Fig. 4](#). The effect of enzyme beads loaded into the system, is similar to the effect of a generic catalyst loading in a chemical reactor: the reaction time is inversely proportional to the loading or, in other words, the conversions and KPIs in different experiments have the same trend as functions of the variable t/m_{enzyme} . Increasing beads loading, reaction time proportionally decreases, while the plateau value of conversion and the peak values of PI are the same as absolute values. Changing the enzyme amount has therefore only an effect on reaction time.

The effect of ethanol concentration on the process requires more considerations. Since in all cases we are working with sub-stoichiometric ethanol (molar ratio < 3), adding ethanol to the

mixture guarantees higher conversion. This higher conversion leads also to a slightly higher PI value, which should make the rich-ethanol cases the most suitable. On the other hand, it is reported in literature that a high concentration of ethanol can lead to enzyme inhibition, as for example obtained in the ethanolysis performed by [Calabrò et al., 2010](#). The same effect can be observed in this work, looking at the first experimental hours, since as the reaction goes ethanol is consumed and inhibition less likely occurs. It is possible to observe how the initial reaction rate - i.e. the slope of the conversion over time curve - is the same at 7% and 9% while it decreases progressively over this value. Although at 13% and 15% it is possible to reach an overall higher PI, it takes about 3–4 times more enzyme to complete the reaction in the same time, for an increase in PI from 1.3 to 1.35. Where enzyme availability can be a limiting factor for the economic of the process, an optimum can be found using 9% of ethanol. In this case, the peak is at 1.3 of PI, that is in turn given by the product of OE resulting 1.48 and TR that is 87.9%. This corresponds to a final ω_3 mass fraction in acylglycerols fraction of 52%, by detaching 12.1% of the initial moles of ω_3 , and therefore losing them as EEs.

4.2. Comparison between SD and UD

In the previous paragraph, the results of the SD have been presented. The SD is able to fit the experimental data with good accuracy and provides a useful tool to predict the ethyl esters production over time depending on enzyme amount and ethanol concentration. This, however, allows to properly describe the ethyl ester fraction and the overall

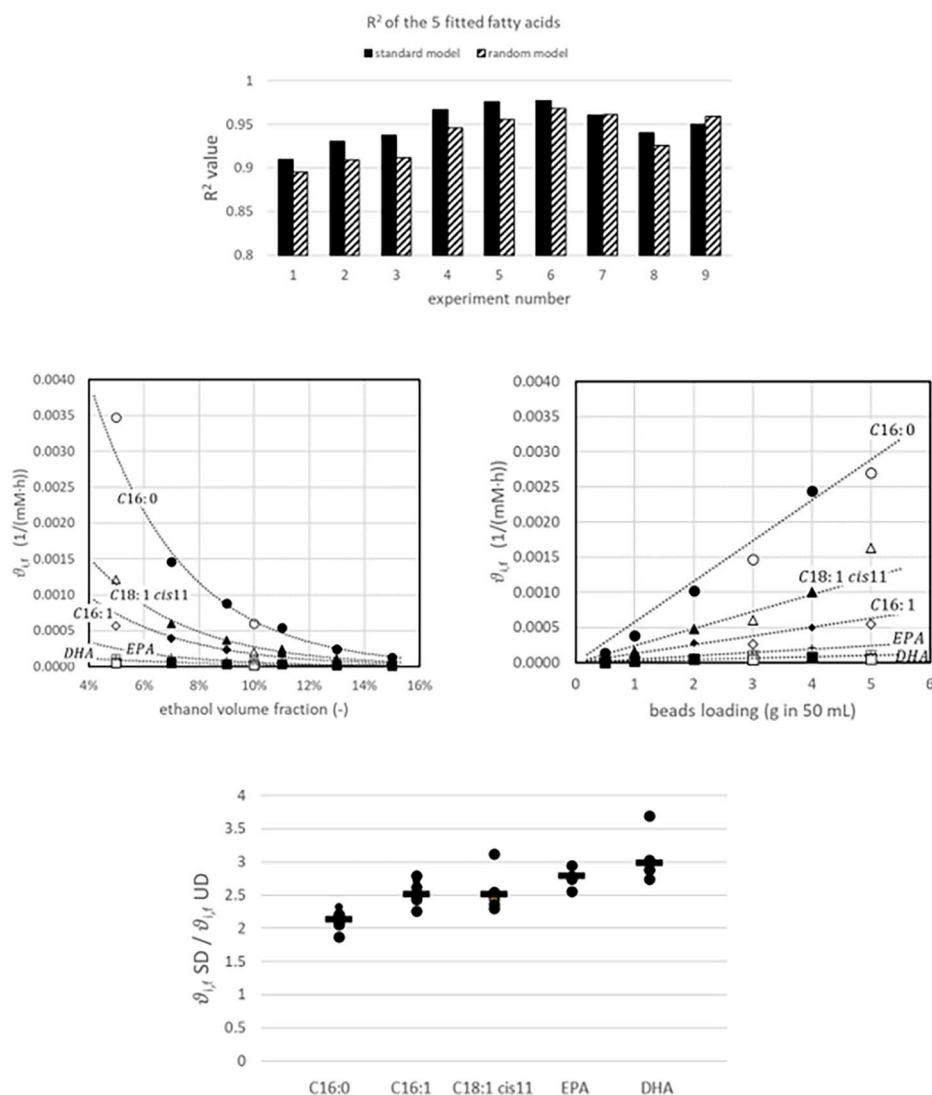


Fig. 5. At the top, R^2 coefficient comparison between the results of the fitting of SD and UD. At the center: on the left, validation of the UD for ethanol concentrations. On the right, validation for enzyme amount. At the bottom, ratio between ϑ_{if} of the SD and UD in the different experiments, with segment indicating average value. (●) C16:0 exp. for fitting; (○) C16:0 exp. for validation; (◆) C16:1 exp. for fitting; (◇) C16:1 exp. for validation; (▲) C18:1cis11 exp. for fitting; (△) C18:1cis11 exp. for validation; (+) EPA exp. for fitting; (⊞) EPA exp. for validation; (■) DHA exp. for fitting; (□) DHA exp. for validation.

acylglycerols fraction, but with potential deviations from reality in the compositions of the different acylglycerols. To overcome this problem and reach a higher accuracy on the final acylglycerols composition, a new acid distribution has been assumed in the model, as described in section 3.3, implemented in Matlab® and used to fit the same experimental data on EEs.

The general trends of concentrations and KPIs are the same as presented in the previous section, since they have been discussed as results of the model but are actually based on the experimental measurements. The focus of this section is mainly to underline the differences between the UD and the SD, rather than to explain again the trends obtained.

4.2.1. UD parameters fitting

As conducted in 4.1.2 for the SD, also the UD has been fitted on the experimental data available, representing the concentrations of EEs of the different fatty acids over time. Likewise with the SD, five main fatty acids have been used to fit the model, while the concentrations of the other eight acids have been calculated based on the fitted ones. Fitting and validation of UD model and the comparison between UD and SD fitting and fitted parameters are reported in Fig. 5.

Results of the fitting in terms of R^2 are reported at the top of Fig. 5.

All values are above 0.88, although higher computation time led to a less-optimized solution compared to the SD. The parameters ϑ_{if} and ϑ_{ib} have been fitted for the 5 main acids.

The trends of ϑ_{if} and ϑ_{ib} over ethanol concentration and over enzyme amount have been fitted with a mathematical function (exponential for ethanol and linear for enzyme) and such functions have been used to validate the model on the experiments 10 to 13, following the same procedure used in the SD. At the center of Fig. 5, the results of the fitting and validation of the forward coefficients, while their mathematical expressions can be found in supplementary materials. The mathematical complexity of the model with UD is higher than the SD one, since here 574 components are involved, together with matrixes that assign the probabilities and the possibilities of obtaining one component from another, as presented in section 3.3.2. For this reason, it can be a good procedure to look for a connection between the ϑ_{if} and ϑ_{ib} of the SD and UD, in order to use the results of the SD as first-guess values in the UD. It resulted that there is a relation between the parameters calculated with the different distributions, reported at the bottom of Fig. 5 for the forward reactions parameters. These relations can be easily derived for all parameters from the expressions of ϑ_{if} and ϑ_{ib} reported in and The ratios are approximately between 2 and 3, since

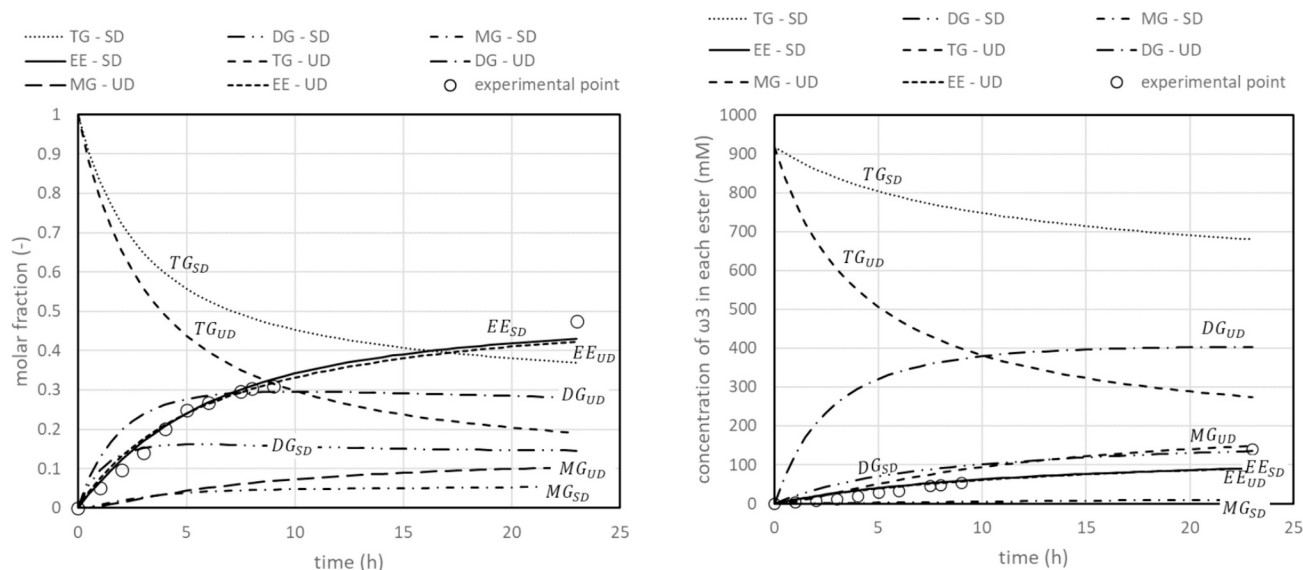


Fig. 6. On the left, comparison between mole fractions of different esters over time for experiment 6 estimated with SD and UD. On the right, comparison between the two models of the $\omega 3$ predicted concentrations in all the ester forms.

in UD the ϑ are related to the acid concentrations, while in SD they are related to the acylglycerols concentration, with a ratio acids/aclyglycerols of 2 for DG and 3 for TG.

4.2.2. Discrepancies in acylglycerols fraction description

Trends of the KPIs are the same observed for the SD, despite the minor differences that may arise from the fitting accuracy, since both models reproduce the same experimental data. The aim of this analysis, however, lays in the verification of how the acylglycerols fraction is described by the two models. On the left of Fig. 6, the molar fractions of the different esters (TGs, DGs, MGs, EEs) over time for one experiment (exp. 6) are reported. As expected, the fraction of EEs computed by the two models is the same, since fitted on the experimental data (white markers in figure). For the acylglycerols (TGs, DGs, MGs), the trends confirm and quantify what was expected: the SD, with its hypothesis that any TGs has only acids of the same type attached, leads to an over-estimation of the TGs in the reaction mixture compared to the UD. DGs and MGs are instead both underestimated, keeping in mind that the total amount of acylglycerols is the same for the two models. Such differences are numerically important and this is evaluated taking the relative difference between predicted UD values compared to predicted SD values, which changes over time, and assuming their median value as representative of the discrepancy. For TG molar fraction, the median of the relative discrepancy moving from SD to UD is 37 %, for DGs -92 % and for MGs -64 %, while for EEs is 2 %. These numbers suggest that the discrepancy between the two assumptions cannot be neglected, and that the necessity of a more accurate model of the initial acids' distribution, as in the UD, should be considered when an accurate description of acylglycerols fraction is required.

This conclusion is even stronger when looking at the $\omega 3$ fatty acids (EPA + DHA) concentration in the different esters, needed to estimate the enrichment of the final product if the separation between acylglycerols and EEs is not 100 % selective. In case some acylglycerols will be lost, and some EEs will remain in the final product, an accurate description of all these fractions allows to estimate the final enrichment. Results are again presented for one experiment, but conclusions are qualitatively general for all the cases investigated. As clear from right side of Fig. 6, the discrepancy is noteworthy. The total molar concentration (and then the moles, since the volume is assumed to be constant) of $\omega 3$ over time is constant and equal to the initial one (acids are only changing ester form). Considering again the median of the relative

discrepancy between SD and UD, for TGs is 51 %, for DGs is 257 % and for MG is 1619 %, while for fitted EEs is 2 %.

5. Conclusions

In this research, fish oil transesterification, performed thanks to a selective lipase, has been performed to produce an acylglycerols fraction enriched in $\omega 3$ fatty acids. A mathematical model has been used to reproduce the experimental data, obtained measuring the ethyl esters produced in the mixture, investigating the effects of enzyme loading and ethanol concentration on reaction performance. Both a selective and a uniform distributions of the acids in the fish oil have been assumed, to investigate their influence on the acylglycerols fraction description, which experimental determination is much more challenging due to the very high number of acylglycerols and acids combinations.

KPIs predicted from the models, while fitted and validated on experimental data, showed that enzyme loading has only an effect on reaction time, while keeping the absolute values and trends of KPIs constant. Increasing ethanol concentration, on the other hand, increases also the maximum PI and conversion. However, above 9 % ethanol shows an inhibition effect, where - to perform the reaction in the same time - 4/5 times the enzyme loading is required to reach the PI peak, while only increasing the maximum from 1.3 to 1.35. Therefore, a good conclusion can be to operate with 9 % of ethanol. In that case, the PI peak is found after 4.5 h with 2 g of beads, where it can increase or decrease inversely proportional to the enzyme loading. The peak of PI is a value of 1.3, given by the product of oil enrichment of 1.35 and a target recovery of 87.9 %. These values correspond respectively to an $\omega 3$ mass fraction in acylglycerols fraction of 52 % (starting from 35 % of the initial oil) and to a loss of $\omega 3$ in the acylglycerols fraction, due to their conversion in EEs, of 12.1 %.

The limits on the conventional assumptions of the selective distribution (where only acids of the same type are attached to a specific acylglycerol), as can be found in literature, have been pointed out, and an alternative version of the model has been proposed, based on a uniform distribution of the fatty acids in the available positions on the triacylglycerols of the fish oil. This new assumption has been used to reproduce the same experimental data and the results of the two models' assumptions have been compared. While leading to a maximum error of 2 % on EEs fitting, therefore sharing the same conclusions on overall description of EEs and acylglycerols fraction as a whole, the descriptions

of the composition of the acylglycerols fraction strongly differs. Inconsistencies can be both found in the prediction of the concentration of the different acylglycerols (TG, DG, MG), from 37 % to 92 % of absolute relative differences, and in the consequent description of the ω 3 concentrations in each fraction. In the latter case discrepancies reached relative values from 51 % for TG up to over 1600 % for MGs.

The improvements in the acylglycerols fraction predictions may have a relevant impact in the process design of ω 3 enrichment, as it can be showed through a couple of examples. The first is about the bioavailability of the product: in Dyerberg et al., 2010, the authors showed that re-esterified acylglycerols had a higher availability compared to, in turn, free fatty acids, natural fish oil and ethyl esters. This higher bioavailability was potentially attributed to the fact that re-esterified products have also both DG and MG content (about 40 %) that could facilitate their absorption in the intestine. In the same manner, an ω 3 enriched product containing the target acid in DG and MG fraction may represent a more valuable product, thus leading to the necessity to a more accurate prediction on their content. A second example is about the second section of the enrichment process, which is the removal of EEs, depleted in ω 3 acids. Among the various separation techniques, this can be done using a membrane separation process. As stated in Marchetti et al., 2014, membrane separation in nanofiltration depends on solute-solvent-membrane interactions, which is affected by both solute diameter and polarity. Having different polarity and diameters, TGs, DGs and MGs may have different permeabilities, and then a correct estimation of their amount may be fundamental in an overall process description, whether membrane technology is used for oil enrichment (Ghasemian et al., 2017).

From this study, it can be concluded that the SD is a powerful and simple tool, which use is suggested every time the requirements of the study are to understand how external conditions (temperature, ethanol concentration, pressure, etc.) influence the ethyl-esters detachment and composition. Nevertheless when, beyond EEs, also detailed information on the acylglycerols fraction is needed but it is technically challenging to perform experimental measurements to determine their amount and their acids content, using the SD can lead to important overestimation of the TGs fraction (and the amount of a certain component in it, accordingly) and a severe underestimation of the DGs and MGs fractions. When such information is required, a more accurate description of the acids' distribution should be used. Since the real distribution has a very high level of complexity, the UD has been proposed to give a more realistic representation of the situation. The results with the UD showed the limits of the SD description, and its usage is recommended whenever information of acylglycerols and their composition is needed. Further development of this study might deal with the validation of kinetics prediction based on experimental determination of acids distribution in acylglycerols fraction over time.

CRedit authorship contribution statement

M. Ongis: Writing – original draft, Validation, Methodology, Investigation, Formal analysis, Conceptualization. **D. Liese:** Writing – review & editing, Investigation, Formal analysis. **G. Di Marcoberardino:** Writing – review & editing, Methodology, Investigation. **F. Gallucci:** Writing – review & editing, Validation, Supervision. **M. Binotti:** Writing – review & editing, Validation, Investigation, Conceptualization.


Declaration of competing interest

The authors declare that they have no known competing financial interests or personal relationships that could have appeared to influence the work reported in this paper.

Data availability

The data that has been used is confidential.

Acknowledgments

 This project has received funding from the European Union's Horizon 2020 Research and Innovation Program under grant agreement No. 869896 (MACBETH).

ChiralVision B.V. is acknowledged for the enzyme formulation and immobilization on the beads. Solutex Corp. is acknowledged for supply of the fish oil.

Appendix A. Supplementary data

Supplementary data to this article can be found online at <https://doi.org/10.1016/j.foodchem.2024.141379>.

References

- Akanbi, T. O., & Barrow, C. J. (2017). Candida antarctica lipase a effectively concentrates DHA from fish and thraustochytrid oils. *Food Chemistry*, 229(February), 509–516. <https://doi.org/10.1016/j.foodchem.2017.02.099>
- Bucio, S. L., et al. (2015). Kinetic study for the ethanolysis of fish oil catalyzed by Lipozyme® 435 in different reaction media. *Journal of Oleo Science*, 64(4), 431–441. <https://doi.org/10.5650/jos.ess14263>
- Calabrò, V., et al. (2010). Kinetics of enzymatic trans-esterification of glycerides for biodiesel production. *Bioprocess and Biosystems Engineering*, 33(6), 701–710. <https://doi.org/10.1007/s00449-009-0392-z>
- Cha, S. (1968). A simple method for derivation of rate equations for enzyme-catalyzed reactions under the rapid equilibrium assumption or combined assumptions of equilibrium and steady state. *Journal of Biological Chemistry*, 243(4), 820–825. [https://doi.org/10.1016/s0021-9258\(19\)81739-8](https://doi.org/10.1016/s0021-9258(19)81739-8)
- Chen, Y., et al. (2022). 'lipase-catalyzed two-step hydrolysis for concentration of acylglycerols rich in ω -3 polyunsaturated fatty acids'. *Food Chemistry*, 400, Article 134115. <https://doi.org/10.1016/j.foodchem.2022.134115>
- Deng, W., et al. (2023). Effect of omega-3 polyunsaturated fatty acids supplementation for patients with osteoarthritis: A meta-analysis. *Journal of Orthopaedic Surgery and Research*, 18(1), 1–11. <https://doi.org/10.1186/s13018-023-03855-w>
- Dighiri, I. M., et al. (2023). Effects of Omega-3 polyunsaturated fatty acids on brain functions: A systematic review. *Cureus*, 9(1), 1–11. <https://doi.org/10.7759/cureus.30091>
- Dong, S., et al. (2023). Preparation of a novel healthy tiger nut oil-based margarine fat with low trans and saturated fatty acids. *Food Chemistry*, 427(June), Article 136731. <https://doi.org/10.1016/j.foodchem.2023.136731>
- Dyerberg, J., et al. (2010). Bioavailability of marine n-3 fatty acid formulations, Prostaglandins, Leukotrienes, and Essential Fatty Acids. *Controlled Clinical Trial*, 83(3), 137–141. <https://doi.org/10.1016/j.plefa.2010.06.007>
- Fiori, L., Manfredi, M., & Castello, D. (2014). Supercritical CO2 fractionation of omega-3 lipids from fish by-products: Plant and process design, modeling, economic feasibility. *Food and Bioprocess Processing*, 92(2), 120–132. <https://doi.org/10.1016/j.fbp.2014.01.001>
- Fiori, L., et al. (2017). From fish waste to Omega-3 concentrates in a biorefinery concept. *Waste and Biomass Valorization*, 8(8), 2609–2620. <https://doi.org/10.1007/s12649-017-9893-1>
- Ghasemian, S., et al. (2017). Omega-3 PUFA concentration by a novel PVDF nano-composite membrane filled with nano-porous silica particles. *Food Chemistry*, 230, 454–462. <https://doi.org/10.1016/j.foodchem.2017.02.135>
- Gog, A., et al. (2012). Biodiesel production using enzymatic transesterification - current state and perspectives. *Renewable Energy*, 39(1), 10–16. <https://doi.org/10.1016/j.renene.2011.08.007>
- He, Y., et al. (2016). Rationale behind the near-ideal catalysis of Candida antarctica lipase a (CAL-A) for highly concentrating ω -3 polyunsaturated fatty acids into monoacylglycerols. *Food Chemistry*, 219, 230–239. <https://doi.org/10.1016/j.foodchem.2016.09.149>
- Jain, P., et al. (2023). Concentrating omega-3 fatty acids in Nannochloropsis oceanica oil by using enzyme immobilized nano-silica systems. *Journal of Cleaner Production*, 406(April), Article 137030. <https://doi.org/10.1016/j.jclepro.2023.137030>
- Jiang, C., et al. (2023). Enzymatic enrichment of acylglycerols rich in n - 3 polyunsaturated fatty acids by selective methanolysis: Optimization and kinetic studies. *Journal of Food Science*, 88(7), 2858–2869. <https://doi.org/10.1111/1750-3841.16618>
- Johnson, K. A., & Goody, R. S. (2011). The original Michaelis constant: Translation of the 1913 Michaelis-Menten paper. *Biochemistry*, 50(39), 8264–8269. <https://doi.org/10.1021/bi201284u>
- Khorshidi, M., et al. (2023). Effect of omega-3 supplementation on lipid profile in children and adolescents: A systematic review and meta-analysis of randomized clinical trials. *Nutrition Journal*, 22(1), 1–11. <https://doi.org/10.1186/s12937-022-00826-5>
- King, B. E. L., & Altman, C. (1956). *A schematic method of deriving the rate laws for enzyme-catalyzed reactions*. *J am chemical society [preprint]*.
- Lei, Q., Ba, S., Zhang, H., Wei, Y., Lee, J. Y., & Li, T. (2015). Enrichment of omega-3 fatty acids in cod liver oil via alternate solvent winterization and enzymatic

- interesterification. *Food Chemistry*, 199, 364–371. <https://doi.org/10.1016/j.foodchem.2015.12.005>
- Lessard, L. P., & Hill, C. G. (2000a). Effect of pH on the production of lipolyzed butter oil by a calf pregastric esterase immobilized in a hollow-fiber reactor: I. Uniresponse kinetics. *Biotechnology and Bioengineering*, 69(2), 183–195. [https://doi.org/10.1002/\(SICI\)1097-0290\(20000720\)69:2<183::AID-BIT7>3.0.CO;2-2](https://doi.org/10.1002/(SICI)1097-0290(20000720)69:2<183::AID-BIT7>3.0.CO;2-2)
- Lessard, L. P., & Hill, C. G. (2000b). Effect of pH on the production of Lipolyzed butter oil by a calf Pregastric esterase immobilized in a hollow-Fiber reactor: II. Multiresponse kinetics. *Biotechnology and Bioengineering*, 69(2), 183–195. [https://doi.org/10.1002/\(SICI\)1097-0290\(20000720\)69:2<183::AID-BIT7>3.0.CO;2-2](https://doi.org/10.1002/(SICI)1097-0290(20000720)69:2<183::AID-BIT7>3.0.CO;2-2)
- Macbeth Consortium. (2019). Macbeth Project. Available at: <https://www.macbeth-project.eu/>.
- Malcata, F. X., Hill, C. G., & Amundson, C. H. (1992). Hydrolysis of butteroil by immobilized lipase using a hollow-fiber reactor: Part II. Uniresponse kinetic studies. *Biotechnology and Bioengineering*, 39(11), 1097–1111. <https://doi.org/10.1002/bit.260391105>
- Marchetti, P., et al. (2014). Molecular separation with organic solvent nanofiltration: A critical review. *Chemical Reviews*, 114(21), 10735–10806. <https://doi.org/10.1021/cr500006j>
- Marsol-Vall, A., et al. (2022). Green technologies for production of oils rich in n-3 polyunsaturated fatty acids from aquatic sources. *Critical Reviews in Food Science and Nutrition*, 62(11), 2942–2962. <https://doi.org/10.1080/10408398.2020.1861426>
- Michaelis, V. L., & Menten, M. L. M. (1913). Die Kinetik der Invertinwirkung. *Journal of the Chemical Society*, 333–369 (February).
- Shahidi, F., & Ambigaipalan, P. (2018). Omega-3 polyunsaturated fatty acids and their health benefits. *Annual Review of Food Science and Technology*, 9, 345–381. <https://doi.org/10.1146/annurev-food-111317-095850>
- Torres, C. F., Hill, C. G., & Otero, C. (2004). Lipase-catalyzed ethanolysis of borage oil: A kinetic study. *Biotechnology Progress*, 20(3), 756–763. <https://doi.org/10.1021/bp034290+>
- Torres, C. F., Moeljadi, M., & Hill, C. G. (2003). Lipase-catalyzed ethanolysis of fish oils: Multi-response kinetics. *Biotechnology and Bioengineering*, 83(3), 274–281. <https://doi.org/10.1002/bit.10667>
- Torres, C. F., et al. (2002). Catalytic transesterification of corn oil and tristearin using immobilized lipases from thermomyces lanuginosa JAOCS. *Journal of the American Oil Chemists' Society*, 79(8), 775–781. <https://doi.org/10.1007/s11746-002-0558-7>
- Ulus, N. N. (2015). Evolution of enzyme kinetic mechanisms. *Journal of Molecular Evolution*, 80(5–6), 251–257. <https://doi.org/10.1007/s00239-015-9681-0>
- Yang, Z., et al. (2020). Enzymatic enrichment of n-3 polyunsaturated fatty acid glycerides by selective hydrolysis. *Food Chemistry*, 346, Article 128743. <https://doi.org/10.1016/j.foodchem.2020.128743>
- Zhang, H., et al. (2023). Association between intake of the n-3 polyunsaturated fatty acid docosahexaenoic acid (n-3 PUFA DHA) and reduced risk of ovarian cancer: A systematic Mendelian randomization study. *Clinical Nutrition*, 42(8), 1379–1388. <https://doi.org/10.1016/j.clnu.2023.06.028>